Performance Comparison of Different Observers for Pendubot

Amjad J. Humaidi[a]*, Abdullah A. Mohammed[b]

*a,b*Department of control and system engineering, University of Technology, Baghdad-10001, Iraq

*a*Email: 601116@uotechnology.edu.iq

*b*Email: Abdullah.ali24@yahoo.com

Abstract

The aim of the work is to study the robust characteristics and performance of four different observers when used to estimate the states of underactuated mechanical system (Pendubot). This work include four observation techniques for state estimation which are Extended State Observer (ESO), nonlinear extended state observer (NESO), Linear Extended State Observer (LESO) and High gain observer (HGO). The Extended State Observer is a model independent observer which includes (NESO, LESO and ESO); it is used for state disturbance observation beside state observation and it has been applied to many practical applications. HGO has a special design of the observer gain that makes it robust to the uncertainties of the nonlinear functions. The effectiveness of each observer is evaluated in terms of its tracking speed and the variance of estimation error which is produced when the system is subjected to noise, disturbance and uncertainties. The observers performances are compared based on simulations using MATLAB package. The simulation results showed that NESO outperforms the other observers where it could give better robust characteristics under noise and uncertainty.

Keywords: Pendubot; ESO; NESO; LESO; HGO.

1. Introduction

The state observers have shown their effectiveness in different applications of many dynamical systems such as detecting, regulation, fault diagnosis, system monitoring, and failures identifying. The main drawback usually reported for most observers is their dependence on mathematical model of system.

----

* Corresponding author.

Therefore, the design of observers have faced critical challenges in practical applications due to the presence of nonlinearities, disturbances and dynamic uncertainties. Thus, obtaining high-performance robust observer design was the target of many researchers. In the last two decades, several advanced observer design techniques have been proposed like high gain observers (HGOs), sliding mode observers (SMO), disturbance observers (DO), extended state observer (ESO), nonlinear extended state observer (NLESO) and linear extended state observer (LESO) [1, 2]. ESO has been firstly proposed by Huang and Han and it was the basic element of Active Rejection Control (ADRC) which recently found numerous applications in different engineering fields [3]. One may summarize the most powerful features of ESO:

- It can efficiently estimate disturbances, uncertainties and sensor noise.
- It can estimate both uncertainties and disturbances by lumping them as a total disturbance.
- ESO has a simple structure, and it can estimate unmolded dynamics precisely in many cases.
- ESO is used in the control system to estimate and compensate disturbances via a feed-forward cancellation technique.
- ESO can be extended to estimate uncertainties and disturbances for multi-input–multi-output (MIMO) systems as well.

Then, Gao had proposed a class of linear ESOs (LESO) and provided guidance on how to choose the optimal parameters in the controller design [4]. A class of nonlinear extended state observers (NESO) was proposed by J. Han [5] in 1995 as a unique observer design. It is rather independent of a mathematical model of the plants, thus achieving robustness. It was tested and verified in key industrial control problems [6].

A high-gain observer (HGO) was firstly proposed by Khalil and Esfandiari for output feedback control design. It is characterized by its ability to estimate the unmeasured states robustly while asymptotically attenuating the disturbances. Since then it has been used in solving many nonlinear system problems [7].

Pendubot has been taken as a case study for observers to be tested. The Pendubot control problem is to swing it up to its vertical unstable equilibrium point (where the two links are in the upright position), and then balance it at that point [8]. for the observation to be applicable, a simple LQR control is used for Pendubot. This would stabilize the unstable state when the two links is at neighborhood of the vertical position; the position nearby the observation is performed [9].

2. Pendubot Model

The pendubot is shown in Figure (1). The first link is displaced with a given θ_1 while the second link displaced with an angle of θ_2. The initial points are $\theta_1 = {}^{-\pi}/_2$ and $\theta_2 = 0$ at the downward position.

One can establish the equations governing the dynamic model of pendubot as follows [10]:

$$[a_1 + a_2 + 2\,a_3\,\cos\theta_2]\,\ddot{\theta}_1 + [a_2 + a_3\,\cos\theta_2]\,\ddot{\theta}_2 - 2\,a_3\,\sin\theta_2\,\dot{\theta}_1\,\dot{\theta}_2 - a_3\,\sin\theta_2\,\dot{\theta}_2^2$$
$$- (-g\,a_4\cos\theta_1 - g\,a_5\cos(\theta_1 + \theta_2)) = \tau \tag{1}$$

$$[a_2 + a_3 \cos\theta_2] \ddot{\theta}_1 + a_2 \ddot{\theta}_2 - a_3 \sin\theta_2 \dot{\theta}_1 \dot{\theta}_2 - \left(-a_3 \sin\theta_2 \dot{\theta}_1^2 - a_3 \sin\theta_2 \dot{\theta}_1 \dot{\theta}_2 - g\, a_5 \cos(\theta_1 + \theta_2)\right)$$
$$= 0 \tag{2}$$

and

$$a_1 = J_1 + m_1 r_1^2 m_2 l_1^2, \; a_2 = J_2 + m_2 r_2^2, \; a_3 = m_2 l_1 r_2, \; a_4 = m_1 r_1 + m_2 l_1, \; a_5 = m_2 r_2.$$

where θ_1 and θ_2 are the angular positons of two links respectively, $\dot{\theta}_1$ and $\dot{\theta}_2$ are the angular velocities of the two links respectively, $\ddot{\theta}_1$ and $\ddot{\theta}_2$ are the angular acceleration of the two links respectively, l_1 and l_2 are the total length of the two links respectively, J_1 and J_2 are the total moment of inertia of the two links respectively, m_1 and m_2 are the total weight of both links respectively, r_1 and r_2 are the distance from the axis of rotation to the center of gravity of the two links respectively, τ is the input torque to the system and g is the gravity.
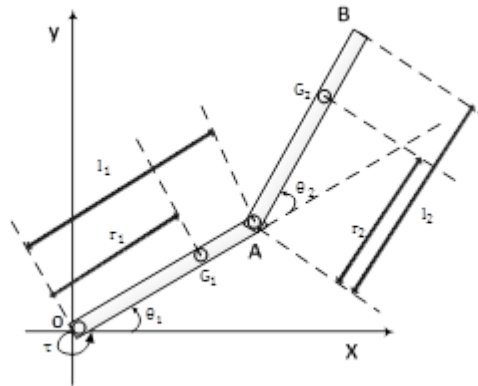

Figure 1: Simplified model of the Pendubot system.

Setting the state variables $x_1 = \theta_1$, $x_2 = \dot{\theta}_1$, $x_3 = \theta_2$ and $x_4 = \dot{\theta}_2$, the compact form of state space for the linearized system, around up-right position at which $(\theta_1, \dot{\theta}_1, \theta_2, \dot{\theta}_2) = (\pi/2, 0, 0, 0)$, can be given as [10], where A and B matrices are found using Jacobian [10].

$$\begin{bmatrix} \theta_1 \\ \dot{\theta}_1 \\ \theta_2 \\ \dot{\theta}_2 \end{bmatrix} = \begin{bmatrix} \dfrac{\partial f_1}{\partial \theta_1} & \dfrac{\partial f_1}{\partial \theta_2} & \dfrac{\partial f_1}{\partial \theta_3} & \dfrac{\partial f_1}{\partial \theta_4} \\ \dfrac{\partial f_2}{\partial \theta_1} & \dfrac{\partial f_2}{\partial \theta_2} & \dfrac{\partial f_2}{\partial \theta_3} & \dfrac{\partial f_2}{\partial \theta_4} \\ \dfrac{\partial f_3}{\partial \theta_1} & \dfrac{\partial f_3}{\partial \theta_2} & \dfrac{\partial f_3}{\partial \theta_3} & \dfrac{\partial f_3}{\partial \theta_4} \\ \dfrac{\partial f_4}{\partial \theta_1} & \dfrac{\partial f_4}{\partial \theta_2} & \dfrac{\partial f_4}{\partial \theta_3} & \dfrac{\partial f_4}{\partial \theta_4} \end{bmatrix} \begin{bmatrix} \theta_1 \\ \dot{\theta}_1 \\ \theta_2 \\ \dot{\theta}_2 \end{bmatrix} + \begin{bmatrix} \dfrac{\partial f_1}{\partial \tau} \\ \dfrac{\partial f_2}{\partial \tau} \\ \dfrac{\partial f_3}{\partial \tau} \\ \dfrac{\partial f_4}{\partial \tau} \end{bmatrix} \tau \tag{3}$$

where

$$\frac{\partial f_2}{\partial \theta_2} = \frac{\partial f_2}{\partial \theta_4} = \frac{\partial f_3}{\partial \theta_3} = \frac{\partial f_4}{\partial \theta_2} = \frac{\partial f_4}{\partial \theta_4} = \frac{\partial f_3}{\partial \theta_1} = 0$$

$$\frac{\partial f_1}{\partial \theta_1} = \frac{\partial f_3}{\partial \theta_3} = \frac{\partial f_1}{\partial \tau} = \frac{\partial f_3}{\partial \tau} = \frac{\partial f_1}{\partial \theta_3} = \frac{\partial f_1}{\partial \theta_4} = 0$$

$$\frac{\partial f_2}{\partial \theta_1} = \frac{(a_2 a_4 - a_3 a_5)\, g}{a_1 a_2 - a_3{}^2} , \frac{\partial f_2}{\partial \theta_3} = \frac{-a_3 a_5\, g}{a_1 a_2 - a_3{}^2} , \frac{\partial f_4}{\partial \theta_3} = \frac{a_5\, g\, (a_1 + a_3)}{a_1 a_2 - a_3{}^2}$$

$$\frac{\partial f_3}{\partial \theta_4} = \frac{\partial f_1}{\partial \theta_2} = 1, \ \frac{\partial f_4}{\partial \tau} = \frac{-a_2 - a_3}{a_1 a_2 - a_3{}^2}$$

$$\frac{\partial f_4}{\partial \theta_1} = \frac{a_5 g(a_1 + a_3) - a_4 g(a_2 + a_3)}{a_1 a_2 - a_3{}^2}, \ \frac{\partial f_2}{\partial \tau} = \frac{a_2}{a_1 a_2 - a_3{}^2}$$

The general law used for linearization is

$$\Delta \dot{x} = A\, \Delta x + B\, \Delta u$$

The system become

$$\dot{x} = A\,(x - x_r) + B\,u \tag{4}$$

where x_r is the equilibrium point $[x_r = (\pi/2, 0, 0, 0)]$. Substitute the numerical values from Table (A.1), the following state space can be found

$$\dot{x} = \begin{bmatrix} 0 & 1 & 0 & 0 \\ 35.7868 & 0 & -17.743 & 0 \\ 0 & 0 & 0 & 1 \\ -24.0845 & 0 & 87.0211 & 0 \end{bmatrix} (x - x_r) + \begin{bmatrix} 0 \\ 56.8923 \\ 0 \\ -118.0847 \end{bmatrix} u \tag{5}$$

3. Stabilization of swing up Using LQR Control

The system is stabilized by Linear Quadratic Regulator (LQR) which is an optimal control design technique. The cost function is parameterized by two matrices, Q and R, that weight the state vector and the system input respectively.

Consider the single-input, single-output (SISO) system described by the general state space form [11],

$$\dot{x} = A\, x + B\, u \tag{6}$$

where u is the control input

$$u = -K\, x = -[K_1\ K_2 \dots K_n]\, x \tag{7}$$

The cost function of system (5) is

$$J = \int_0^\infty (x^T Q\, x + R\, u^2)\, dt \tag{8}$$

where R is a scalar weighting factor. The above cost function is minimized when

37

$$K = R^{-1} B^T P \tag{9}$$

the P is $n \times n$ matrix determined by the following equation

$$A^T P + P A - P B R^{-1} B^T P + Q = [0] \tag{10}$$

such that it give $P = P^T > 0$, Q and R are selected such that P give a positive definite.

It can be shown that the system is stabilized by with the following setting of weight matrix Q and R chosen as follows.

$$Q = \begin{bmatrix} 30 & 0 & 0 & 0 \\ 0 & 40 & 0 & 0 \\ 0 & 0 & 60 & 0 \\ 0 & 0 & 0 & 0 \end{bmatrix}, \ R = [1]$$

Then, the elements of the gain matrix can be easily obtained become

$$K = [-113.442 \quad -23.934 \quad -104.85 \quad -14.714]$$

so that the eigenvalues of closed system $|(\lambda I - B K)|$ at unstable equilibrium point become

$$\lambda_1 = -360, \lambda_2 = -7.9134, \lambda_3 = -6.5474 , \lambda_4 = -1.4595$$

4. Development and Design of Observers for pendubot

In what follows, the development of equations describing suggested observers is presented. Also, the observer design is set-up to place the poles of each observer at desired locations. The analysis is initiated by high gain observer (HGO) and then followed by the other three types of extended state observers.

4.1 High gain observer

Let $\hat{x}_1$ represents the estimate of the first link angular position, and then the observer design for the first link of pendubot is based on the following equations

$$e_1 = (x_1 - \hat{x}_1)$$

$$\dot{\hat{x}}_1 = \hat{x}_2 + \frac{\alpha_1}{\varepsilon} e_1 \tag{11}$$

$$\dot{\hat{x}}_2 = \frac{\alpha_2}{\varepsilon^2} e_1$$

where e_1 are the estimation error of the first link position. For the second link, the observer set of equations is

$$e_2 = (x_3 - \hat{x}_3)$$

$$\dot{\hat{x}}_3 = \hat{x}_4 + \frac{\alpha_3}{\varepsilon} \, e_2 \tag{12}$$

$$\dot{\hat{x}}_4 = \frac{\alpha_4}{\varepsilon^2} \, e_1$$

where e_2 are the estimation error of the second link position. The HGO gains are adjusted as [12].

$$h_1 = \frac{\alpha_1}{\varepsilon} \; , h_2 = \frac{\alpha_2}{\varepsilon^2}$$

$$h_3 = \frac{\alpha_3}{\varepsilon} \; , h_4 = \frac{\alpha_4}{\varepsilon^2}$$

where $(\alpha_i \, ; i = 1, .., 4)$ are chosen so that $(A - LC)$ is Hurwitz. They are chosen so that the observer poles would lie in $(-\omega_0)$ at the half-plane

$$\lambda(s) = s^2 + \alpha_1 \, s + \alpha_2 = (s + \omega_0)^2$$

$$\lambda(s) = s^2 + \alpha_3 \, s + \alpha_4 = (s + \omega_0)^2$$

by a simple calculation the poles can be obtained

$$\alpha_1 = \alpha_3 = 2 \, \omega_0, \quad \alpha_2 = \alpha_4 = \, \omega_0{}^2$$

where $0 < \varepsilon \ll 1$.

4.2 Extended state observers

In this part, the equations relevant to the three observers (ESO, NESO and LESO) is established and the designs of suggested observers are setup to be next applied for observations of the pendubot system.

4.2.1 Extended state observer

Pendubot observer design for the first link:

$$e_1 = \hat{x}_1 - x_1$$

$$\dot{\hat{x}}_1 = \hat{x}_2 - \frac{\alpha_1}{\varepsilon} \, e_1$$

$$\dot{\hat{x}}_2 = -\frac{\alpha_2}{\varepsilon^2} \, e_1 + b_0 \, u + \hat{x}_5 \tag{13}$$

$$\dot{\hat{x}}_5 = -\frac{\alpha_5}{\varepsilon^3} \, e_1$$

where e_1 are the estimation error of the first link position. On the other hand, the observer structure for the second link:

$$e_2 = \hat{x}_3 - x_3$$

$$\dot{\hat{x}}_3 = \hat{x}_4 - \frac{\alpha_3}{\varepsilon} e_2$$

$$\dot{\hat{x}}_4 = -\frac{\alpha_4}{\varepsilon^2} e_2 + b_0 u + \hat{x}_6 \tag{14}$$

$$\dot{\hat{x}}_6 = -\frac{\alpha_6}{\varepsilon^3} e_2$$

where e_2 is the position estimation error of the second link, b_0 is the normal value of b, (α_i ; $i = 1,..,6$) are chosen so that $(A - LC)$ is Hurwitz. They are chosen so that the observer poles would lie in $(-\omega_0)$ at the half-plane [12].

$$\lambda(s) = s^3 + \alpha_1 s^2 + \alpha_2 s + \alpha_5 = (s + \omega_0)^3$$

$$\lambda(s) = s^3 + \alpha_3 s^2 + \alpha_4 s + \alpha_6 = (s + \omega_0)^3$$

then, it is easy to calculate α_i in terms of frequency ω_0

$$\alpha_1 = \alpha_3 = 3\,\omega_0, \qquad \alpha_2 = \alpha_4 = 3\,{\omega_0}^2, \qquad \alpha_5 = \alpha_6 = {\omega_0}^3$$

To eliminate peaking phenomenon, the parameter (ε) is made to be varying with time such that $\varepsilon = 1/R(t)$ and the function $R(t)$ given by [13]

$$R = \left[\begin{array}{ll} 100\,t^3 & 0 \le t \le 1 \\ 100 & t > 1 \end{array} \right. \tag{15}$$

if noise or disturbance act on the practical measurement signal very small (ε) will cause big observer error. To eliminate the effect of noise or disturbance, a switched gain can be used at the observer in the case of observers used in control design of the system.

4.2.1 Nonlinear Extended State Observer (NESO):

The observer design for pendubot are represented below. The observer equations of the first link is given by

$$e_1 = \hat{x}_1 - x_1$$

$$\dot{\hat{x}}_1 = \hat{x}_2 - \beta_1 \, \text{fal}\,(e_2, \alpha_1, \sigma)$$

$$\dot{\hat{x}}_2 = \hat{x}_5 - \beta_2 \, \text{fal}\,(e_2, \alpha_2, \sigma) + b_0 u \tag{16}$$

$$\dot{\hat{x}}_5 = -\beta_5 \, \text{fal}\,(e_2, \alpha_5, \sigma)$$

where e_1 is the position estimation error of the first link. For the second link, the observer structure is as

follows:

$$e_2 = \hat{x}_3 - x_3$$

$$\dot{\hat{x}}_3 = \hat{x}_4 - \beta_3 \ \text{fal} \ (e_2, \alpha_3, \sigma)$$

$$\dot{\hat{x}}_4 = \hat{x}_6 - \beta_4 \ \text{fal} \ (e_2, \alpha_4, \sigma) + b_0 \ u \tag{17}$$

$$\dot{\hat{x}}_6 = -\beta_6 \ \text{fal} \ (e_2, \alpha_6, \sigma)$$

where e_2 is the position estimation error of the second link, b_0 is the normal value of b, $(A - LC)$ must be Hurwitz, β is adjastibule gain, b_0 is the normal value of B, and *fal (.)* is defined as [12]:

$$\text{fal}(e, \alpha, \sigma) = \begin{cases} |e|^\alpha \ sign(e), |e| > \sigma \\ \dfrac{e}{\sigma^{1-\alpha}}, \qquad |e| \leq \sigma \end{cases} \tag{18}$$

where $\sigma > 0$. The nonlinear function is used to make the observer more efficient, was selected heuristically based on experimental results. The *fal* function are represented in Figure (2).
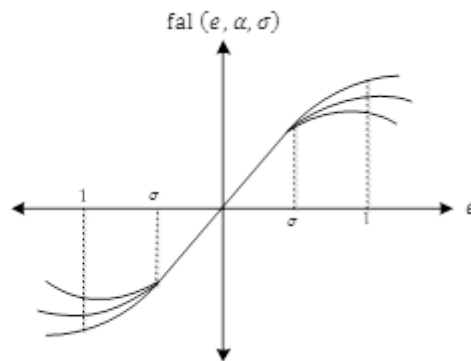
Figure 2: Linear and nonlinear function.

The observer gains designated by elements of matrix $L = [\beta_1, \beta_2, \beta_3, \beta_4, \beta_5, \beta_6]$ are chosen so that the observer poles would lie in $-\omega_0$ at the half-plane [12].

$$\lambda(s) = s^3 + \beta_1 \ s^2 + \beta_2 \ s + \beta_5 = (s + \omega_0)^3$$

$$\lambda(s) = s^3 + \beta_3 \ s^2 + \beta_4 \ s + \beta_6 = (s + \omega_0)^3 \ \text{Then}$$

$$\beta_1 = \beta_3 = 3 \ \omega_0, \beta_2 = \beta_4 = 3 \ {\omega_0}^2, \beta_5 = \beta_6 = {\omega_0}^3$$

where ω_0 are chosen so that it could be a trade-off between how fast the observer tracks the states and how sensitive it is to the sensor noises.

4.2.3 Linear Extended Observer (LESO)

The main difference between NESO and LESO is that LESO works in the linear part of fal function and no nonlinearity is included within its descriptive equations. For Pendubot, the observer equations of the first link is given by

$$e_1 = \hat{x}_1 - x_1$$

$$\dot{\hat{x}}_1 = \hat{x}_2 - \beta_1\, e_1$$

$$\dot{\hat{x}}_2 = \hat{x}_5 - \beta_2\, e_1 + b_0\, u \qquad\qquad (19)$$

$$\dot{\hat{x}}_5 = -\beta_5\, e_1$$

where e_1 are the estimation error of the first link position. On the other hand, the observer equations for the second link is given by

$$e_2 = \hat{x}_3 - x_3$$

$$\dot{\hat{x}}_3 = \hat{x}_4 - \beta_3\, e_2$$

$$\dot{\hat{x}}_4 = \hat{x}_6 - \beta_4\, e_2 + b_0\, u \qquad\qquad (20)$$

$$\dot{\hat{x}}_6 = -\beta_6\, e_2$$

where $(A - LC)$ must be Hurwitz. Observer gains $L = [\beta_1, \beta_2, \beta_3, \beta_4, \beta_5, \beta_6]$ are chosen so that the observer poles would lie in $-\omega_0$ at the half-plane [12].

$$\lambda(s) = s^3 + \beta_1\, s^2 + \beta_2\, s + \beta_5 = (s + \omega_0)^3$$

$$\lambda(s) = s^3 + \beta_3\, s^2 + \beta_4\, s + \beta_6 = (s + \omega_0)^3$$

then,

$$\beta_1 = \beta_3 = 3\,\omega_0,\ \ \beta_2 = \beta_4 = 3\,\omega_0{}^2,\ \ \beta_5 = \beta_6 = \omega_0{}^3$$

where ω_0 are chosen so that it could be a trade-off between how fast the observer tracks the states and how sensitive it is to the sensor noises.

5. Simulated Results

The designed parameter of HGO, LESO, NESO and ESO, respectively are listed in Tables (A.2), (A.3), (A.4) and (A.5).

The performance comparison of observers is assessed in terms of the speed of tracking and variance of estimation error. The simulation of the pendubot with four cases (nominal, disturbance, noise and uncertainty) are shown below.

5.1 Nominal System

Figure (3) below shows the actual behavior of system states and the estimate states of the observers for the first link of the pendubot. Figure shows the actual state of angular position (x_1) and the estimate state of angular position $(\hat{x}_1)$. Also, the figure depicts the actual state of velocity angular position (x_2) and the estimate state of velocity angular position $(\hat{x}_2)$ resulting from all observers. The error for angular position and its estimate (e_1) and angular velocity and its estimate (e_2) are also indicated in the figure. It is shown in the figure that NESO has the fastest transient response among the other observers but with variance of $e_1 = 0.0011$ and $e_2 = 1.028$ while HGO has the lowest variance of $e_1 = 5.5288e*10^{-4}$ and $e_2 = 0.3664$
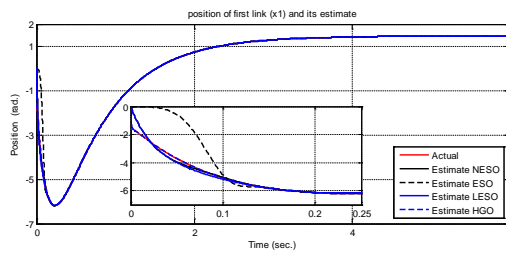

(a)
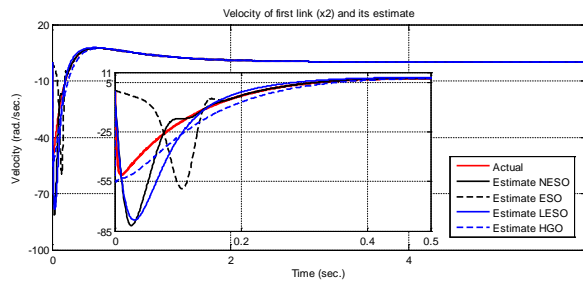
(b)
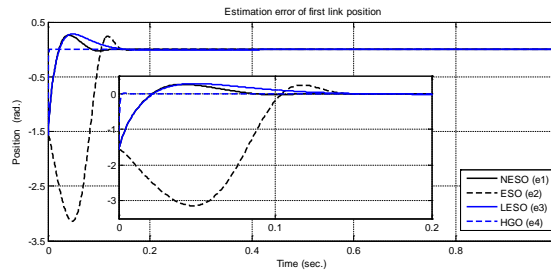
(c)

Figure 3: Actual and estimate states for first link of pendubot system (**Nominal Case**)

Figure (4) gives the actual and estimate responses of the angular position $(x_3, \hat{x}_3)$ and velocity angular position $(x_4, \hat{x}_4)$ for the second link. Also, The error for angular position and its estimate (e_1) and angular velocity and its estimate (e_2) are also shown in the figure. It is clear from the figure that HGO has the fastest and the lowest estimation error with estimation error variance of $e_3 = 3.8341 * 10^{-10}$ and $e_4 = 0.0286$. NESO and LESO also give a good performance with variance of $(e_3 = 2.1071 * 10^{-4}$ and $e_4 = 4.3021)$ for NESO and $(e_3 = 2.7728 * 10^{-4}$ and $e_4 = 5.2348)$ for LESO.
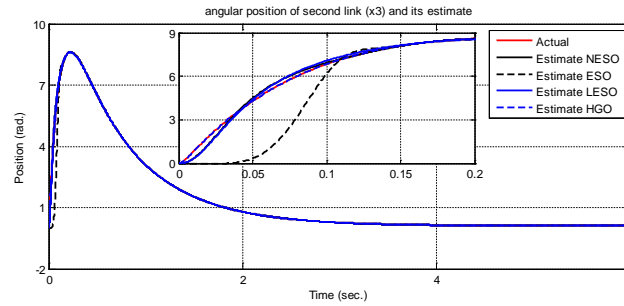
(a)
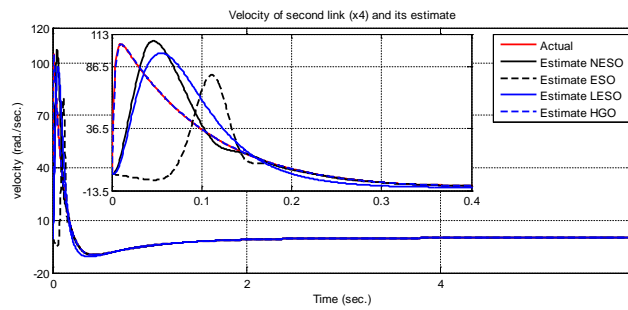
(b)
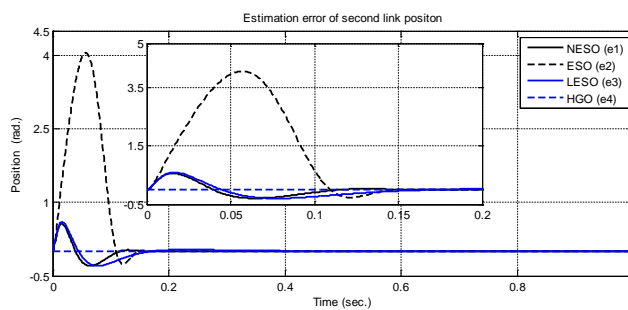
(c)

Figure 4: Actual and estimate states for Pendulum of pendubot system (**Nominal Case**)

Figures (3,4) (a, b and c) clarify the actual response of the Pendubot position with the state estimated by observers and the estimation error of angular position.

5.2 pendubot system under disturbance

In this section, the same set of behaviors shown in previous scenarios are repeated with the system is subjected to disturbance and the performance of observers will be assessed accordingly. The applied disturbance is a pulse of height 0.1, which is exerted at time interval 4-5 seconds during the simulation time.

The same states and estimation errors as before are shown in Figure (5) for the first link part of the system. It has seen that that HGO has the best performance with variance of $e_1 = 0.0020$ and $e_2 = 0.4333$. Also NESO shows a good performance with variance of $e_1 = 0.0025$ and $e_2 = 1.2661$.
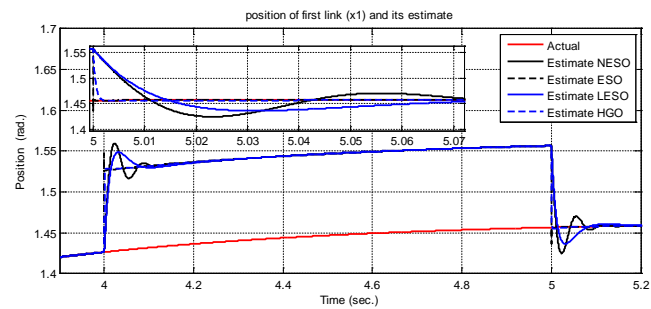

(a)
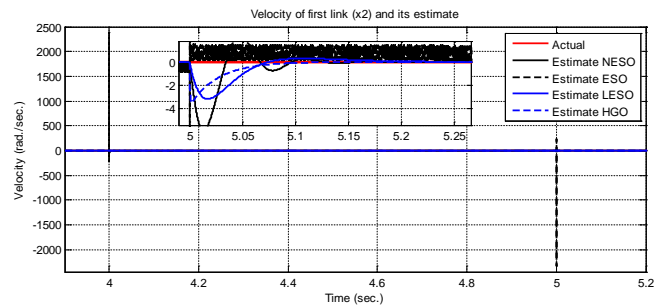
(b)
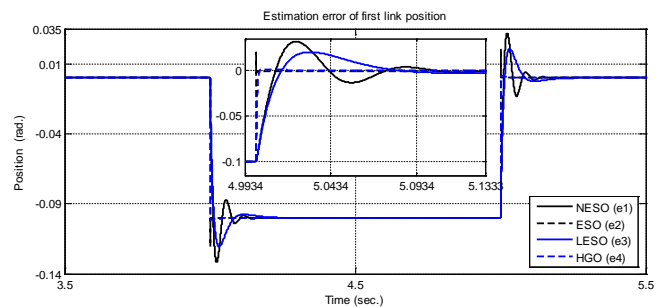
(c)

Figure 5: Actual and estimate states for the first link of pendubot system (**Under Disturbance**)

For the second link part, the simulations illustrated in Figure (6). It is clear that HGO has a fast transient response with variance of e_3 =0.0015 and e_4 =7.4083. NESO has a slow transient but it has the lowest variance of its estimation error of e_3 =0.0017 and e_4 =4.5411.
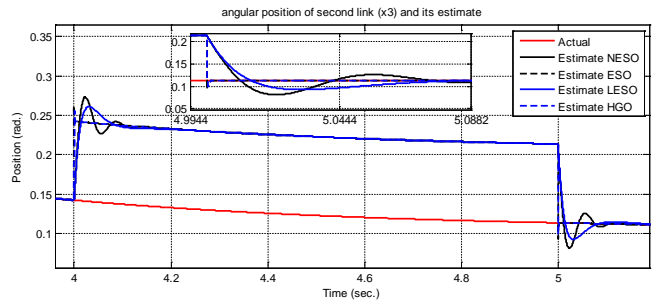

(a)
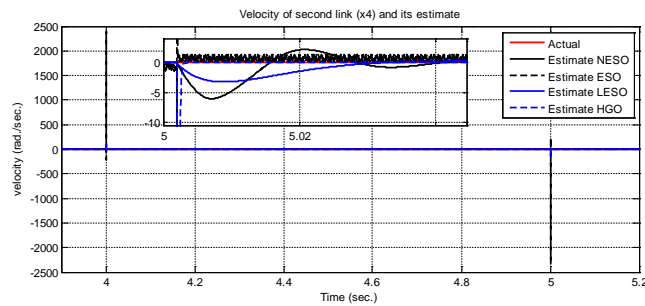
(b)
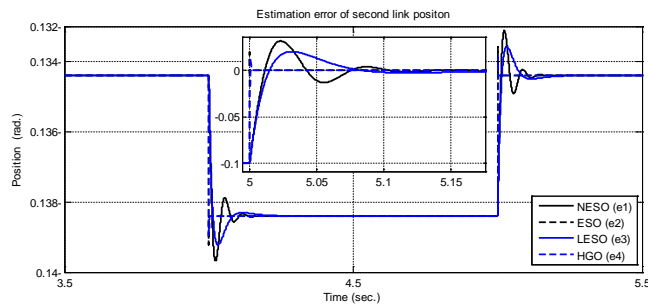
(c)

**Figure 6:** Actual and estimate states for arm of second link system (**Under Disturbance**)

Figures (5, 6) (a, b and c) clarify the actual response of the Pendubot with the state estimated by observers and the estimation error of angular position when an input disturbance is applied to the system.

5.2 pendubot system with noise

In what follows, the performance of observers is assessed again when the system is injected with noise at both

links. A white noise power of 6 and 20 are imposed to first and second link, respectively.

Figure (7) illustrate the actual response of the first link, the responses of estimated states and estimation errors for position and velocity for all observers. The figure shows that NESO has the best performance for the first link it has a fast transient response and low variance of $e_1 = 0.0011$ and $e_2 = 1.1604$. Also HGO shows a good performance and its variance is $e_1 = 5.4996 * 10^{-4}$ and $e_2 = 2.0963$.
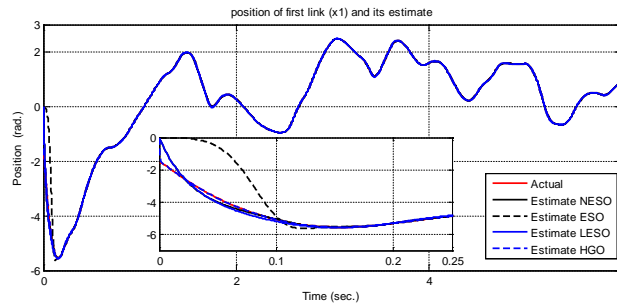

(a)
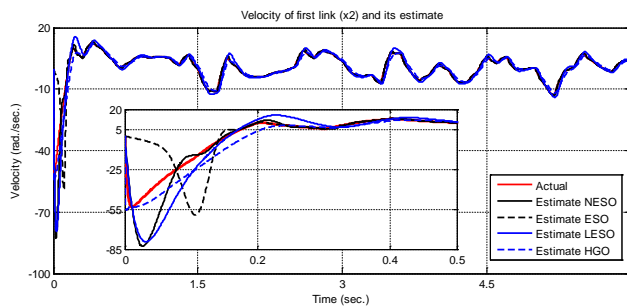
(b)
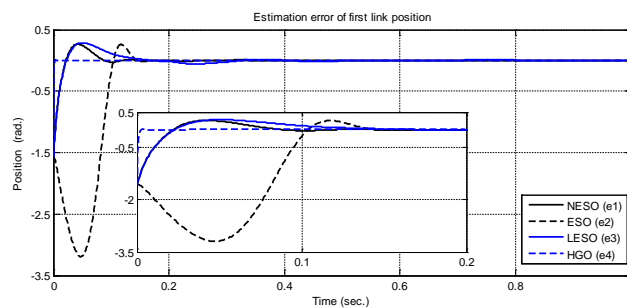
(c)

Figure 7: Actual and estimate states for first link of pendubot system (**with noise injection**)

The second link response with its estimated states and error are illustrated in Figure (8). The simulation shows that HGO has a better response than the other observers it has the fastest transient response and the lowest variance of $e_3 = 3.8798 * 10^{-10}$ and $e_4 = 0.0284$. NESO also shows a fast transient response and low

estimation error variance of $e_3 = 2.5021 * 10^{-4}$ and $e_4 = 5.0226$.
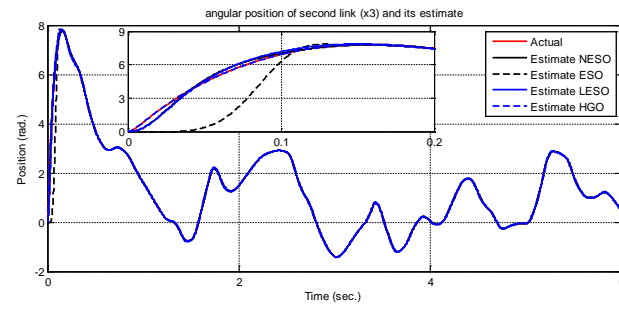

(a)
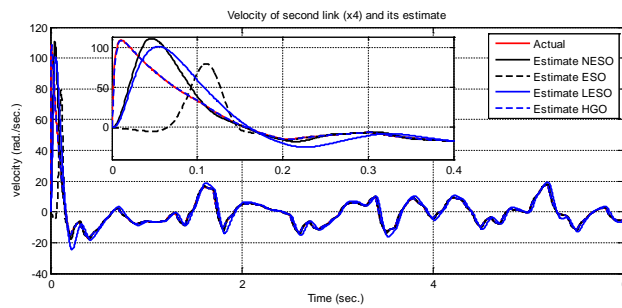
(b)
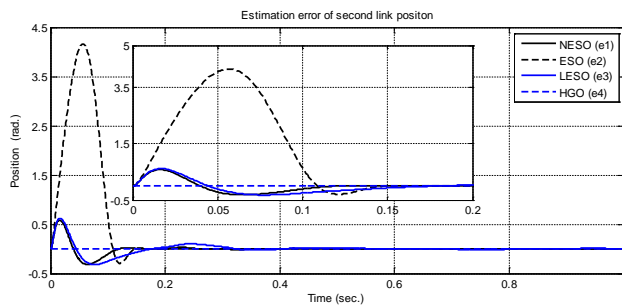
(c)

Figure 8: Actual and estimate states for second link of pendubot system (**with noise injection**)

Figures (7, 8) (a, b and c) clarify the actual response of the Pendubot with the state estimated by observers and the estimation error of angular position when an input disturbance is applied to the system.

5.4 pendubot system with Uncertainty

It is assumed that the system has uncertainty in load moment of inertia such that its value will increase 100% over the nominal value. Figure (9) shows the responses of actual and estimated states and also the estimation error for both angular position and velocity for the first link of pendubot. It is evident from the figure that, HGO

has the lowest estimation error variance of $e_1 = 5.4999 * 10^{-4}$ and $e_2 = 1.6434$ and its transient response is good but the fastest one is NESO with variance of $e_1 = 0.0012$ and $e_2 = 3.0165$. ESO also has a fast response than HGO but its variance is largest one $e_1 = 0.0272$ and $e_2 = 10.9321$.
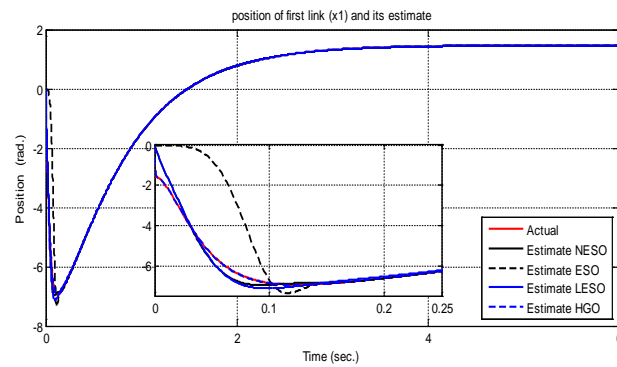
(a)
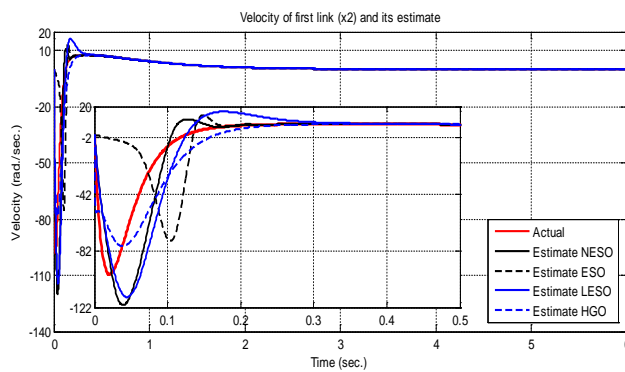
(b)
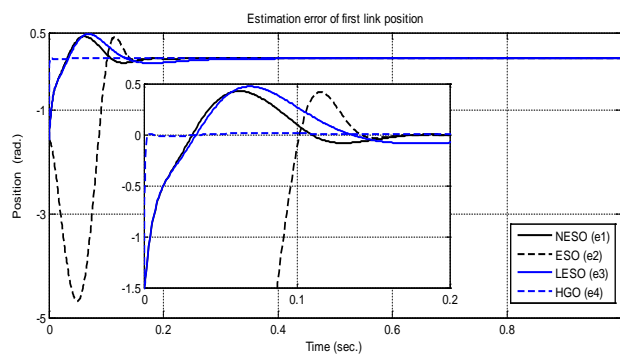
(c)

Figure 9: Actual and estimate states for first link of pendubot system (**with uncertainty**)

According to the figure (10), that HGO has the best performance and its variance is $e_3 = 3.3969 * 10^{-10}$ and $e_4 = 0.0233$. NESO also has a good performance and its variance is $e_3 = 8.9734 * 10^{-4}$ and $e_4 = 16.1226$.
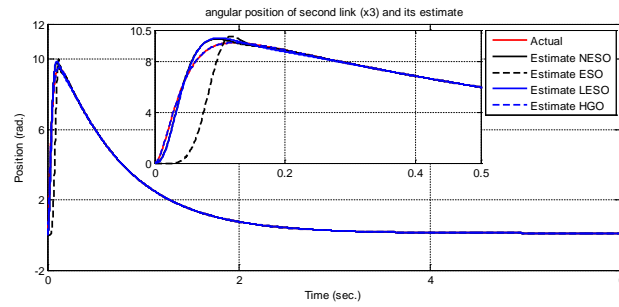
(a)
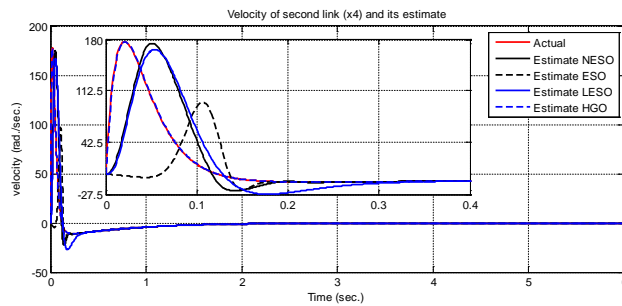
(b)
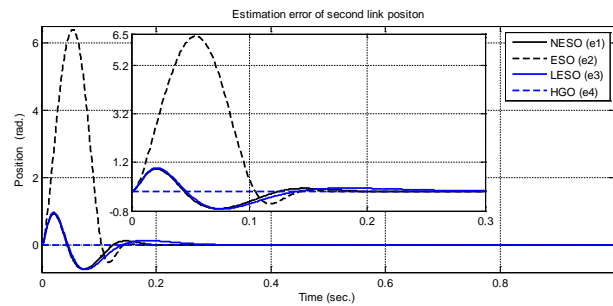
(c)

Figure 10: Actual and estimate states for second link of pendubot system (**with uncertainty**)

6. Conclusion

The simulation shows that there is no unique observer could cope with all systems uncertainties, noises and disturbances for both links of pendubot.

This is due to the structure characterized each observer. As it has been reported using simulation, for every case and for every link, there is salient observer outperforms the others in terms of minimum variance and high dynamic performance. However, on the average, the NESO showed good dynamic characteristics with low variances.

HGO shows a good transient response. ESO shows a peaking phenomenon under disturbance. LESO and NESO perform approximately the same for the nominal system and the system under disturbance.

Reference

[1]. W. Wang, "A Comparative Study of Nonlinear Observers and Control Design Strategies", Ph.D. dissertation, Dept. Elect. Eng., Cleveland state university, 2003.

[2]. W.R.AbdulAdheem, I.K.Ibraheem, "Improved Sliding Mode Nonlinear Extended State Observer based Active Disturbance Rejection Control for Uncertain Systems with Unknown Total Disturbance", International Journal of Advanced Computer Science and Applications, 2016, Vol. 7, No. 12, PP.80-93.

[3]. Han, J., "From PID to active disturbance rejection control", IEEE Transactions on Industrial Electronics, 2009, 56, (3), PP. 900–906.

[4]. Z. Gao, S. Hu and F. Jiang. "A novel motion control design approach based on active disturbance rejection", Proceedings of the 40th IEEE Conference on Decision and Control, Orlando, Florida USA, December 2001, pp: 4877-4882.

[5]. J. Han, "A class of extended state observers for uncertain systems", Control and Decision, Vol.10, No.1, pp: 85-88, 1995.

[6]. Y. Hou, et al. "Active disturbance rejection control for web tension regulation'. Proceedings of the 40th IEEE Conference on Decision and Control, Orlando, Florida USA, December 2001, pp. 4974-4979.

[7]. F. Esfandiari and H.K. Khalil. "Output feedback stabilization of fully linearizable systems", International Journal of Control, 1992, pp. 1007:1037.

[8]. M.W. Spong, D.J. Block, "The Pendubot: A mechatronic system for control research and education", Proc. of the 34th IEEE Conference on Decision and Control, pp. 555–556, 1995.

[9]. N.D quyen, N. van thuyen, "Rotary Inverted Pendulum and Control of Rotary Inverted Pendulum by Artificial Neural Network", National Conference on Theoretical Physics, 2012, vol.37 , pp. 243-249.

[10]. Isabelle Fantoni, Lozano Rogelio, "Non-linear Control for Underactuated Mechanical Systems", springer verlage london, france, 2002.

[11]. V. Sirisha and Dr. Anjali. S. Junghare, "A Comparative study of controllers for stabilizing a Rotary Inverted Pendulum", International Journal of Chaos, Control, Modelling and Simulation (IJCCMS), India, DOI : 10.5121/ijccms.2014.3201, Vol.3, No.1/2, 2014.

[12]. W.Wang 2003, "A Comparative Study of Nonlinear Observers and Control Design Strategies", for degree of doctorate of engineering, Cleveland State University, 2003.

[13]. Jinkun Liu, Xinhua Wang, "Advanced Sliding Mode Control for Mechanical Systems", Tsinghua University Press, Beijing and Springer-Verlag, Berlin Heidelberg, 2012.

[14]. Dufour Aurelie, et.al. " Final REPORT Pendubot", Royal Institute of Technology, 2006.

Appendix

Table (A.1) lists the parameter values of pendubot [14]. Table (A.2-A.5) gives the design parameters obtained for each observer.

Table (A.1): The numeric values of pendubot parameters

Parameter	Symbol	Value	Unit
The total moment of inertia link(1)	J_1	$8.03 * 10^{-3}$	$Kg.m^2$
Total length of the link (1)	l_1	0.21	m
Distance from the axis of rotation of link (1) to the center of gravity	r_1	0.116	m
Total weight of the link (1)	m_1	0.4825	Kg
The total moment of inertia link(2)	J_2	$1.812 * 10^{-3}$	$Kg.m^2$
Total length of the link (2)	l_2	0.233	m
Distance from the axis of rotation of link (2) to the center of gravity	r_2	0.134	m
Total weight of the link (2)	m_2	0.2208	Kg
Gravitational constant	g	9.81	m/s^2

Table (A.2): HGO parameter

Parameter	Value
ω_{02}	40
α_1	20
α_2	7.34
α_3	80
α_4	1600
ε	0.01

Table (A.4): NESO parameter.

Parameter	Value
$\omega_{01} = \omega_{02}$	40
$\beta_1 = \beta_3$	120
$\beta_2 = \beta_4$	4800
$\beta_5 = \beta_6$	64000

$\alpha_1 = \alpha_2$	1
$\alpha_3 = \alpha_4$	0.75
$\alpha_5 = \alpha_6$	0.5

Table (A.3): LESO parameter.

Parameter	Value
$\omega_{01} = \omega_{02}$	300
$\alpha_1 = \alpha_3$	900
$\alpha_2 = \alpha_4$	$27 * 10^4$
$\alpha_5 = \alpha_6$	$27 * 10^6$
ε	0.01

Table (A.5): ESO parameter.

Parameter	Value
$\omega_{01} = \omega_{02}$	40
$\beta_1 = \beta_3$	120
$\beta_2 = \beta_4$	4800
$\beta_5 = \beta_6$	64000